A framework for near-wall RANS/LES coupling

By G. Medic, G. Daeninck†, J.A. Templeton and G. Kalitzin

1. Introduction

In recent years, a lot of effort has been put into combining the Reynolds-averaged Navier Stokes (RANS) technique with large-eddy simulation (LES) in order to reduce its computational cost. One approach is to avoid resolving the near-wall layer altogether by applying wall models which provide wall stress boundary conditions to LES. Such methods have been used by Balaras *et al.* (1996), Cabot & Moin (2000) and Wang & Moin (2000) with some success, although they under-predict the mass flow rate in channel flow. Another approach involves the use of grids coarsened in the wall-parallel direction, while leaving the wall-normal resolution unchanged. Not all turbulent scales can be resolved with such grids and additional modeling is required. RANS equations are well suited for this type of grids because only the mean wall-normal gradients must be resolved while the entire turbulence spectrum is modeled. A well-known approach in this category is detached-eddy simulation (DES) which was designed to simulate massively separated aerodynamic flows. RANS is used in the boundary layer and LES resolves the separated region, see Spalart *et al.* (1997) for more details. However, in pressure-driven channel flow DES over-predicts the mass flow rate, as discussed in Nikitin *et al.* (2000).

A novel concept for the near-wall treatment of LES has been presented in Kalitzin *et al.* (2005b), Medic *et al.* (2005) and Templeton *et al.* (2005). Combined with a wall stress model it has been applied successfully to channel flow at high Reynolds numbers. The near-wall treatment has also been applied with wall-parallel coarsening, which is further investigated in this paper. In the proposed formulation, a RANS eddy-viscosity corrected dynamically using the resolved turbulent stress is imposed near the wall. The RANS eddy-viscosity was precomputed from the RANS equation for channel flow using the averaged velocity profile from the LES and stored in a look-up table.

The details of the near-wall formulation are presented in Section 2. The influence of the RANS turbulence model on the RANS/LES coupling is analyzed in Section 3. First, the results computed with the LES-based precomputed table for the RANS eddy-viscosity are compared to simulations with tables precomputed using the k-ω model of Wilcox (1993) and the Spalart & Allmaras (1994) model. Then it is shown that the RANS eddy-viscosity can also be obtained by solving the RANS turbulence model equations simultaneously with the LES. In Section 4, the influence of the SGS model is analyzed by comparing the results obtained with the WALE model of Nicoud & Ducros (1999) to the dynamic and "classical" Smagorinsky models. The analysis presented in Sections 3 and 4 was carried out for channel flow at $Re_\tau = 395$ on wall-resolved grids and compared to traditional LES. Finally, in Section 5, the proposed formulation is applied on grids coarsened in wall-parallel directions to investigate the possibility of computational savings. The results are presented for channel flow at $Re_\tau = 950$ and detailed comparison is made with DNS results of del Alamo *et al.* (2004).

† Mechanical Engineering Department, Université catholique de Louvain, B-1340 Louvain-la-Neuve, Belgium

2. Near-wall RANS/LES coupling

LES equations for the filtered velocity $\hat{u}_i$ are solved in the entire computational domain:

$$\frac{\partial \hat{u}_i}{\partial t} + \frac{\partial \left(\hat{u}_j \, \hat{u}_i\right)}{\partial x_j} = -\frac{1}{\rho}\frac{\partial \hat{p}}{\partial x_i} + \frac{\partial}{\partial x_j}\left(\left(\nu + \nu_t^{SGS}\right)\frac{\partial \hat{u}_i}{\partial x_j}\right), \tag{2.1}$$

$$\frac{\partial \hat{u}_j}{\partial x_j} = 0. \tag{2.2}$$

In the near-wall region, typically over a dozen of computational cells, the instantaneous SGS eddy-viscosity is replaced by a RANS eddy-viscosity corrected using the resolved turbulent stress:

$$\nu_t^{SGS,NW} = \nu_t^{rans} + \overline{\hat{u}\hat{v}} \,/\, \frac{d\bar{\hat{u}}}{dy}, \tag{2.3}$$

where $\hat{u}$ and $\hat{v}$ are the streamwise and wall-normal velocity components. Since $\overline{\hat{u}\hat{v}}$ and $d\bar{\hat{u}}/dy$ have opposite signs, the second term on the right hand side of (2.3) is negative. Thus, in the presence of turbulent fluctuations, the near-wall LES viscosity, $\nu_t^{SGS,NW}$, is always less than the RANS viscosity, ν_t^{rans}, with the difference being a dynamic correction for the resolved fluctuations. The RANS eddy-viscosity can be obtained from either precomputed look-up tables or from a simultaneous solution of RANS turbulence models. The velocity gradient, $d\hat{u}/dy$, and the turbulent stress, $\hat{u}\hat{v}$, come from the LES. The averaging operator can either be plane- or time-averaging. When using this approach, it is necessary to clip the eddy-viscosity, as is standard practice when using an SGS model, where the eddy-viscosity is clipped whenever its value drops below zero. Here, the eddy-viscosity is clipped at the level of the SGS model. The derivation of equation (2.3) for channel flow and additional discussion can be found in Kalitzin *et al.* (2005b), Medic *et al.* (2005) and Templeton *et al.* (2005).

The RANS and LES models used in the simulations were programmed by G. Daeninck. The flow solver is a modification of the DNS code of Wu & Durbin (2001) which uses a second-order finite-volume method for solving the time-dependent three-dimensional incompressible Navier-Stokes equations in a generalized coordinate system. The approach is based on the scheme developed in Rosenfeld *et al.* (1991), in which volume flux variables (products of the velocity and the face area vectors) are used with the traditional time-splitting fractional step method. The equations are discretized using a staggered mesh system; the pressure is defined at the center of each cell and a volume flux is defined across each face. The method is limited to geometries that are complex in two directions, while the third, spanwise direction must be treated using Cartesian coordinates and periodic boundary conditions. The code allows periodic boundary conditions in the streamwise direction; a source term was added to the momentum equations to enforce a pressure gradient that drives the flow. The pressure gradient can be adjusted dynamically to maintain a constant mass flux through the channel. The k-ω model of Wilcox (1993) and the Spalart & Allmaras (1994) model (see Appendix 1) were considered for the RANS computations; whereas the following subgrid scale models were used for the LES: Wall Adapting Local Eddy-viscosity model (WALE) by Nicoud & Ducros (1999), as well as the dynamic and "classical" Smagorinsky models (for details, see Appendix 2).

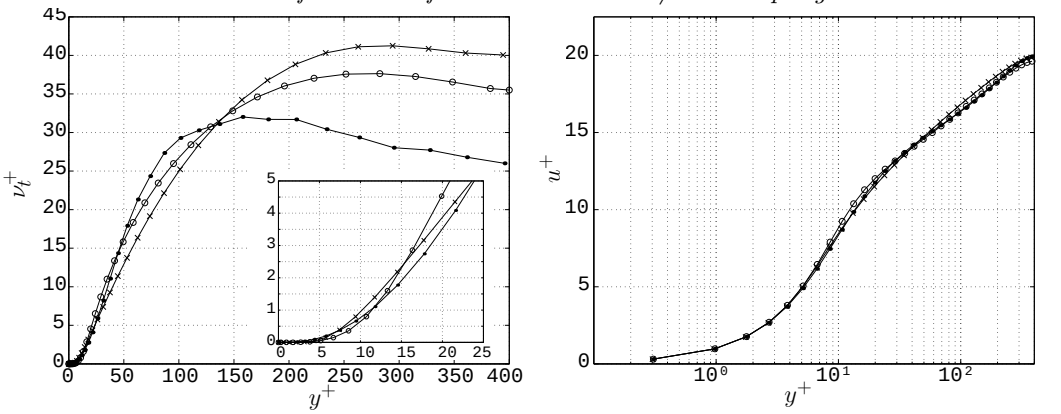

FIGURE 1. Channel flow at $Re_\tau = 395$. Precomputed tables for ν_t^{rans} (left) and the corresponding velocity profiles (right). Computations using ν_t^{rans} from LES (•), Spalart-Allmaras (○) and k-ω turbulence model (×).

3. Influence of the RANS turbulence model

The influence of the RANS turbulence model on the RANS/LES coupling is investigated for plane channel flow at $Re_\tau = 395$. The channel dimensions are $2\pi h \times 2h \times \pi h$. A wall-resolved grid used in the simulations consists of $80 \times 64 \times 64$ cells in the streamwise, wall-normal and spanwise directions, respectively, with the first cell center at $y_1^+ = 0.3$. The WALE subgrid-scale model has been used for the computations presented in this section.

3.1. *Precomputed tables for* ν_t^{rans}

The RANS eddy-viscosity, ν_t^{rans}, used in (2.3) to compute the near-wall eddy-viscosity $\nu_t^{SGS,NW}$, can be stored in precomputed look-up tables. These look-up tables were generated with a method similar to what was used in Kalitzin *et al.* (2005a) for RANS wall functions.

The tables are constructed using several approaches. The first one uses an averaged velocity profile obtained from the resolved LES of channel flow at $Re_\tau = 395$. The look-up table for the eddy-viscosity, $\nu_t^+(y^+)$, is obtained from the non-dimensional RANS equation for channel flow $(1 + \nu_t^+)\, du^+/dy^+ = 1 - y^+/Re_\tau$, where du^+/dy^+ is the gradient of the averaged velocity taken from the LES. This assures that when this eddy-viscosity is used everywhere, the averaged velocity profile from the LES is recovered. Two additional tables were constructed by storing the eddy-viscosity from channel flow RANS computations with Spalart-Allmaras and k-ω models (described in Appendix 1). All three RANS eddy-viscosity and velocity profiles are shown in Fig. 1. Note that even for channel flow, the solutions of these two RANS turbulence models differ from the LES solution.

Next, these RANS eddy-viscosity tables are used to compute $\nu_t^{SGS,NW}$ in the near-wall region of the LES simulation. The near-wall region extends up to $y^+ = 20$ (first 12 cells above the wall). Results computed with these three tables and a wall-resolved LES are presented in Fig. 2. The velocity profiles compare well with the LES. Interestingly, the spread in the velocity profiles for all four simulations is smaller than for the three RANS simulations presented in Fig. 1.

A closer look at the relative error $(u_{LES}^+ - u^+)/u_{LES}^+$ reveals that the computation with the LES-based table has the smallest error in the logarithmic region. However, the error for all simulations is relatively small (less than 1% in the logarithmic layer), which

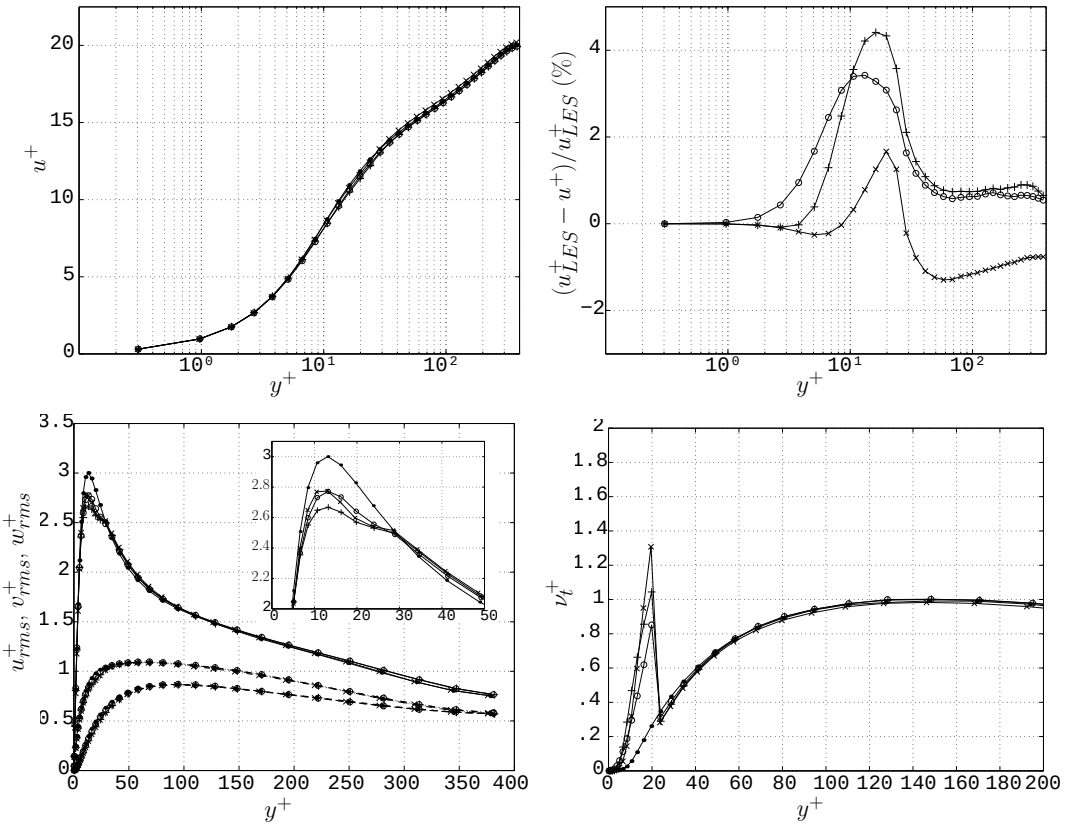

FIGURE 2. Channel flow at $Re_\tau = 395$. Top: u^+ and $(u^+_{LES} - u^+)/u^+_{LES}$ (in %); Bottom: rms velocities and ν_t^+. LES (•); LES + $\nu_t^{SGS,NW}$ with LES-based table for ν_t^{rans} (∘); LES + $\nu_t^{SGS,NW}$ with Spalart-Allmaras table for ν_t^{rans} (×); LES + $\nu_t^{SGS,NW}$ with k-ω table for ν_t^{rans} (+).

suggests that the use of eddy-viscosity coming from RANS turbulence models is appropriate to be used in the proposed approach. Note that the error is largest where the switch from the near-wall treatment to full LES occurs, as shown in the plots for the eddy-viscosity in the same figure. This also affects the peak in the u_{rms} velocity.

3.2. *Dynamic coupling with RANS turbulence model equations*

This section describes the dynamic coupling of LES with RANS turbulence model equations. A RANS turbulence model is solved simultaneously with the LES simulation; the LES provides an averaged velocity $\bar{\tilde{u}}$ that is used to compute the convection and production terms in the RANS turbulence model equations. For example, for the k-ω model the equations are:

$$\frac{\partial k}{\partial t} + \bar{\tilde{u}}_j \frac{\partial k}{\partial x_j} = P_k - C_\mu \omega k + \frac{\partial}{\partial x_j}\left((\nu + \sigma_k \nu_t) \frac{\partial k}{\partial x_j} \right), \tag{3.1}$$

$$\frac{\partial \omega}{\partial t} + \bar{\tilde{u}}_j \frac{\partial \omega}{\partial x_j} = \frac{\gamma \omega}{k} P_k - \beta \omega^2 + \frac{\partial}{\partial x_j}\left((\nu + \sigma_\omega \nu_t) \frac{\partial \omega}{\partial x_j} \right), \tag{3.2}$$

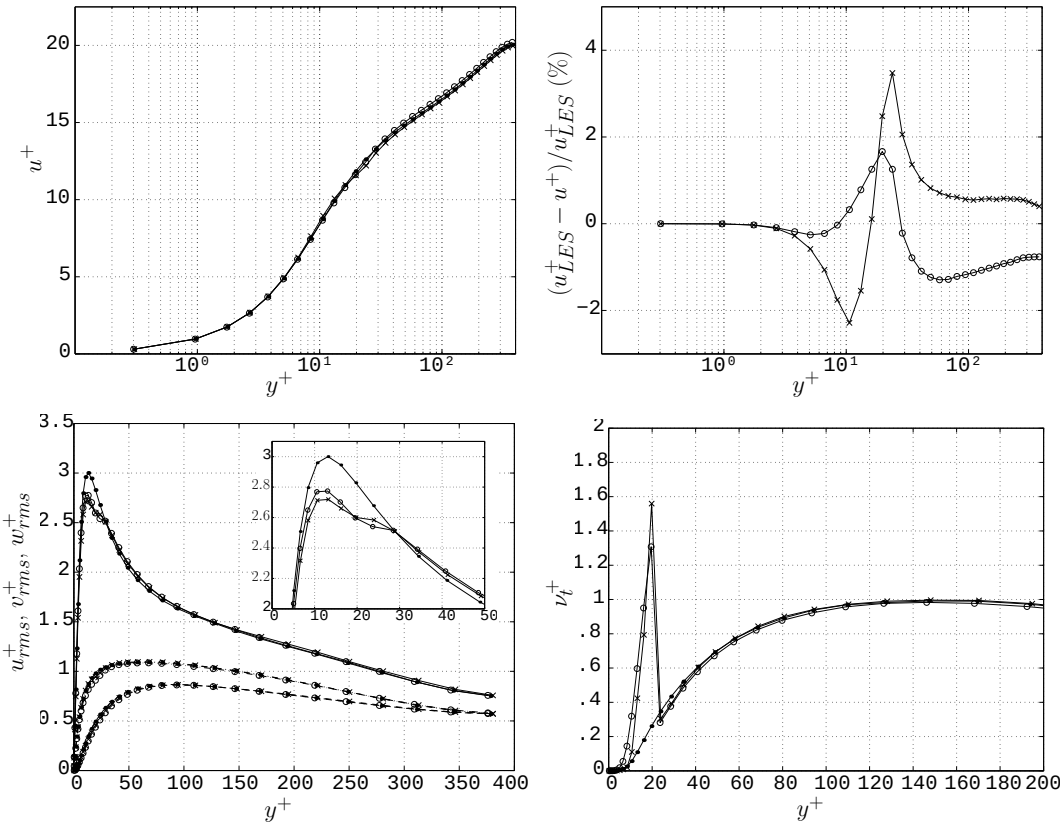

FIGURE 3. Channel flow at $Re_\tau = 395$. Top: u^+ and $(u^+_{LES} - u^+)/u^+_{LES}$ (in %); Bottom: rms velocities and ν_t^+. LES (•); LES + $\nu_t^{SGS,NW}$ with Spalart-Allmaras table for ν_t^{rans} (○); LES + $\nu_t^{SGS,NW}$ with dynamic coupling with Spalart-Allmaras model equations (×).

$$P_k = 2\,\nu_t\,S_{ij}S_{ij}, \qquad S_{ij} = \frac{1}{2}\left(\frac{\partial \bar{\tilde{u}}_i}{\partial x_j} + \frac{\partial \bar{\tilde{u}}_j}{\partial x_i}\right). \tag{3.3}$$

In the case of channel flow, it is convenient to use plane-averaging to compute $\bar{\tilde{u}}$. The RANS turbulence model provides ν_t^{rans}, which is then used to compute $\nu_t^{SGS,NW}$ for the near-wall region in the LES, according to (2.3).

Results for LES simulations using Spalart-Allmaras turbulence model for the near-wall treatment are presented in Fig. 3. The results obtained with the precomputed table and the dynamic coupling with the model equations are compared to a wall-resolved LES. The difference in the results obtained with two approaches is negligible. However, as can be seen from the relative error for u^+, a stronger variation is observed near the switching point when the dynamic coupling is used.

Results for the near-wall treatment with k-ω turbulence model are presented in Fig. 4. Again, the results obtained with the precomputed table and the dynamic coupling with the model equations are compared to a wall-resolved LES. Similarly to Spalart-Allmaras results, the differences are small. Interestingly, the dynamic coupling produces a smaller jump in the eddy-viscosity at the switching location, and the u_{rms} velocity is slightly closer to the wall-resolved LES.

The stress balance presented in Fig. 5 reveals that the resolved stress computed with

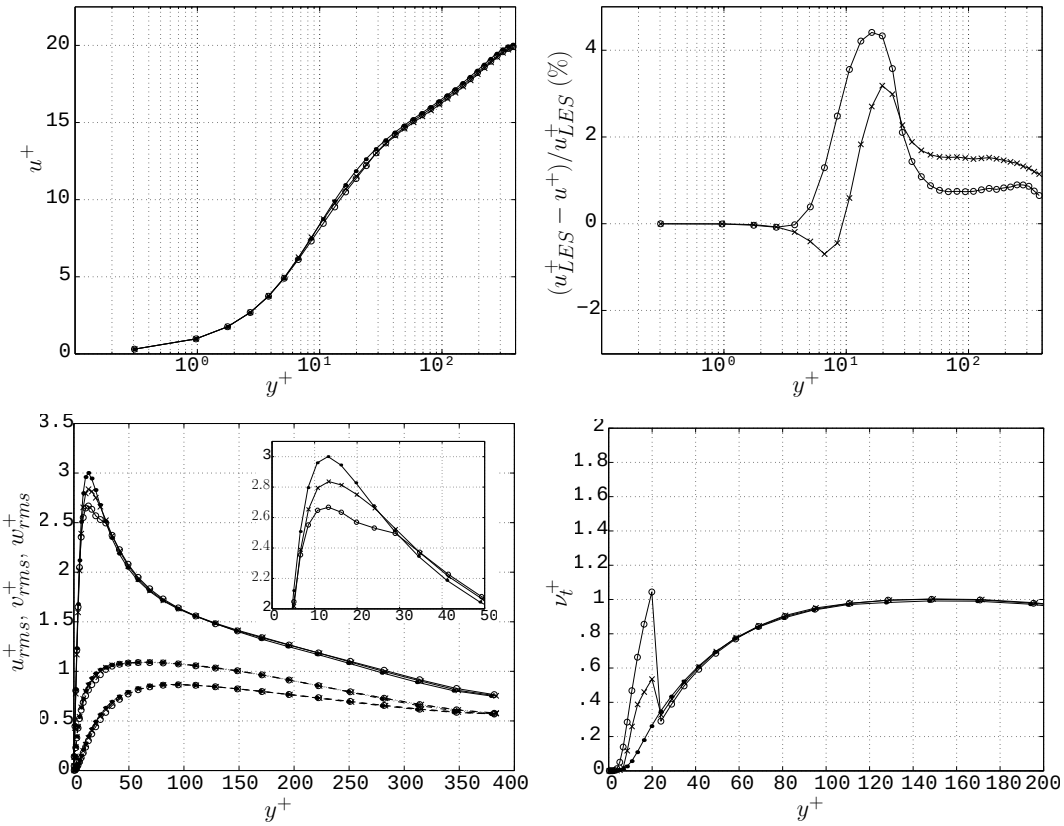

FIGURE 4. Channel flow at $Re_\tau = 395$. Top: u^+ and $(u^+_{LES} - u^+)/u^+_{LES}$ (in %); Bottom: rms velocities and ν_t^+. LES (•); LES + $\nu_t^{SGS,NW}$ with k-ω table for ν_t^{rans} (○); LES + $\nu_t^{SGS,NW}$ with dynamic coupling with k-ω model equations (×).

the dynamic coupling with the k-ω model equations in the near-wall region practically coincides with the results from the LES. The isosurfaces of the instantaneous streamwise vorticity computed using the same approach are also presented in the same figure. These plots illustrate that the near-wall treatment does not affect the LES nature of the simulation.

Note that the dynamic coupling of LES with RANS turbulence model equations was also tested without the correction (2.3), i.e by applying directly the RANS eddy-viscosity, ν_t^{rans}, in the near-wall region. In such computations, the abrupt changes in the mean velocity profile at the switching location (at $y^+ = 20$) were more pronounced, leading to an excess production of turbulence and numerical instabilities. A result for the Spalart-Allmaras model is presented in Fig. 6. This indicates that the correction with the resolved stress in (2.3) is a key element in the coupling procedure.

4. Influence of the subgrid-scale model

The influence of the subgrid scale model on RANS/LES coupling is analyzed in this section. The computations are performed with the dynamic and "classical" Smagorinsky model using $\nu_t^{SGS,NW}$ in the near-wall region (with ν_t^{rans} from precomputed tables).

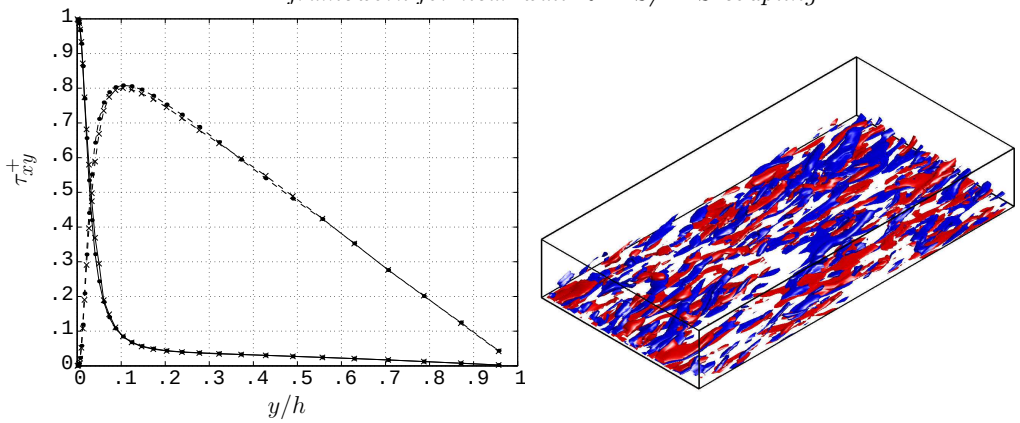

FIGURE 5. Channel flow at $Re_\tau = 395$. Stress balance (left) and isosurfaces of instantaneous streamwise vorticity ω_x (right). LES (•); LES + $\nu_t^{SGS,NW}$ with dynamic coupling with k-ω model equations (×).

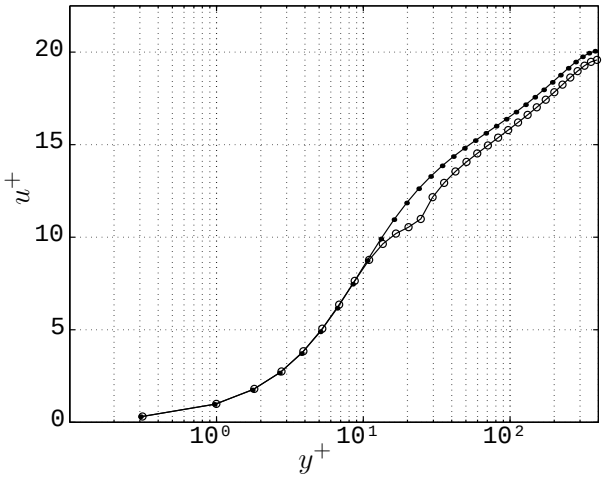

FIGURE 6. Channel flow at $Re_\tau = 395$. Mean velocity u^+. LES (•); LES dynamically coupled with Spalart-Allmaras model without the correction in equation (2.3) (○).

The"classical" Smagorinsky model was intentionally used here with the constant coefficient, $C_s = 0.18$, with no damping functions near the wall.

4.1. *Dynamic Smagorinsky model (DSM)*

The results for the dynamic Smagorinsky model are presented in Fig. 7. Full LES is compared to computations that employ a near-wall treatment for $\nu_t^{SGS,NW}$: (i) using precomputed LES-based table for ν_t^{rans}, (ii) using Spalart-Allmaras table for ν_t^{rans} and (iii) using k-ω table for ν_t^{rans}. The near-wall region for all three computations extends up to $y^+ = 20$ (first 12 cells above the wall).

Overall, the results are very similar to the results obtained with the WALE model presented in Fig. 2. The velocity profiles computed with all three tables compare well with the LES. The relative error, $(u^+_{LES} - u^+)/u^+_{LES}$, is relatively small for all simulations (less than 1% in the logarithmic layer). As for computations with WALE SGS model,

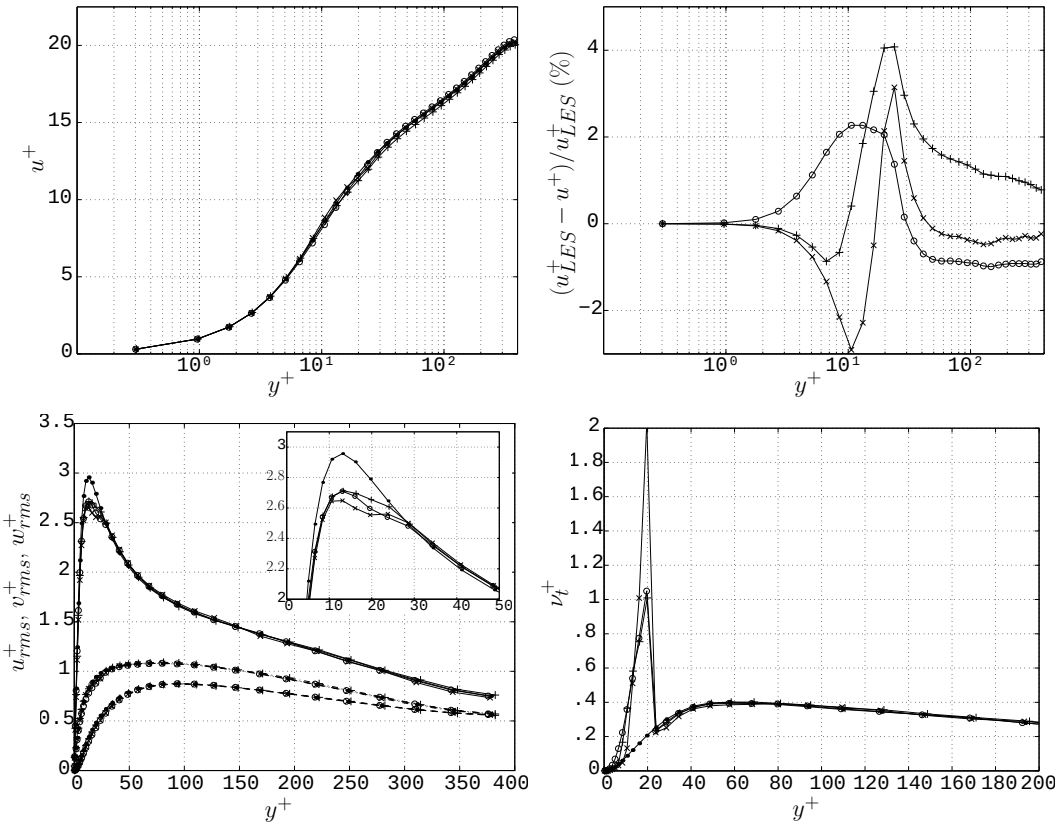

FIGURE 7. Channel flow at $Re_\tau = 395$. Top: u^+ and $(u^+_{LES} - u^+)/u^+_{LES}$ (in %); Bottom: rms velocities and ν_t^+. LES/DSM (•); LES/DSM + $\nu_t^{SGS,NW}$ with LES-based table for ν_t^{rans} (○); LES/DSM + $\nu_t^{SGS,NW}$ with Spalart-Allmaras table for ν_t^{rans} (×); LES/DSM + $\nu_t^{SGS,NW}$ with k-ω table for ν_t^{rans} (+).

the error is largest where the switch from the near-wall treatment to full LES occurs, as shown in the plots for the eddy-viscosity in the same figure. This also affects the peak in the u_{rms} velocity.

4.2. *"Classical"Smagorinsky model*

The "classical" Smagorinsky model is known to fail in the near-wall region, as shown in Fig. 8. It significantly under-predicts the mean-velocity profile, as well as the rms velocities. This is due to the incorrect behavior of the eddy-viscosity in the near-wall region. The results significantly improve if the "classical" Smagorinsky model is used with the proposed near-wall treatment; the eddy-viscosity is now reduced to zero at the wall. Note that the near-wall region extends here up to $y^+ = 80$ ($y/h = 0.2$).

5. Computational savings through wall-parallel coarsening

The previous sections offers a proof of concept for the proposed RANS/LES coupling. For this approach to allow computational savings over the traditional wall-resolved LES, it must be applicable to coarser grids. If the no-slip boundary conditions are to be used, only limited coarsening in the wall-normal direction can be applied. Thus, savings must

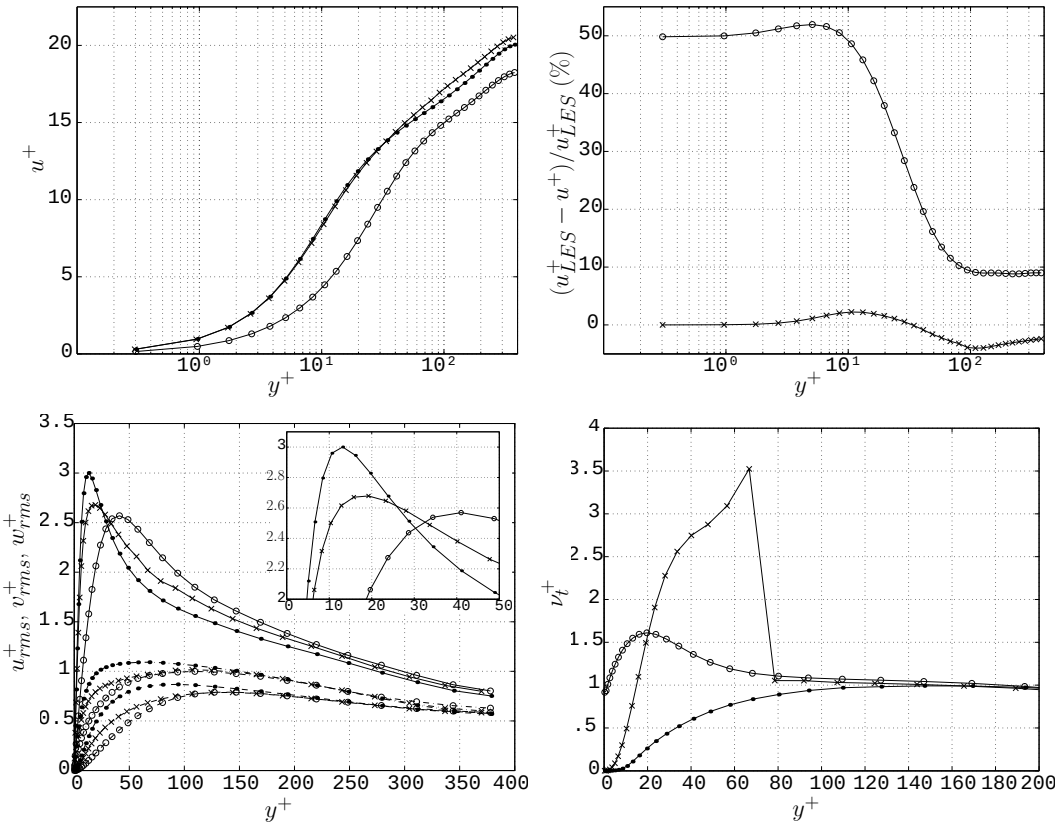

FIGURE 8. Channel flow at $Re_\tau = 395$. Top: u^+ and $(u^+_{LES} - u^+)/u^+_{LES}$ (in %); Bottom: rms velocities and ν_t^+. LES with WALE model (•); LES with "classical" Smagorinsky model (○); LES with "classical" Smagorinsky model + $\nu_t^{SGS,NW}$ with LES-based table for ν_t^{rans} (×).

be achieved through wall-parallel coarsening; a similar philosophy is used in DES; see Nikitin *et al.* (2000).

Wall-parallel coarsening is analyzed for the channel flow at $Re_\tau = 950$ and compared to DNS results of del Alamo *et al.* (2004). Both the proposed near-wall treatment for LES dynamically coupled with the k-ω model and the traditional LES are used on a grid with $64 \times 64 \times 64$ cells and $y_1^+ = 0.7$. The SGS model in these computations is the WALE model, and the near-wall treatment is applied up to $y^+ = 50$ (approximately $y/h = 0.05$).

The requirements on the grid spacing in the wall-parallel directions can be related to spanwise spacing of streamwise streaks; see for example Kline *et al.* (1967). It has been suggested that the grid spacing in the spanwise direction should not exceed 50 plus units. The grid used here matches that criterion.

The results are presented in Fig. 9. When the traditional LES is used on a grid this coarse, the mean velocity is significantly over-predicted. In contrast, the results with the near-wall treatment agree much better with the DNS. As already observed in previous computations with wall-parallel coarsening at $Re_\tau = 395$ with $32 \times 129 \times 32$ cells, presented in Medic *et al.* (2005), the differences in the rms velocities are more significant. The near-wall treatment improves the results when compared to the traditional LES, but the near-wall peak in the u_{rms} velocity is still over-predicted. The increase of the near-

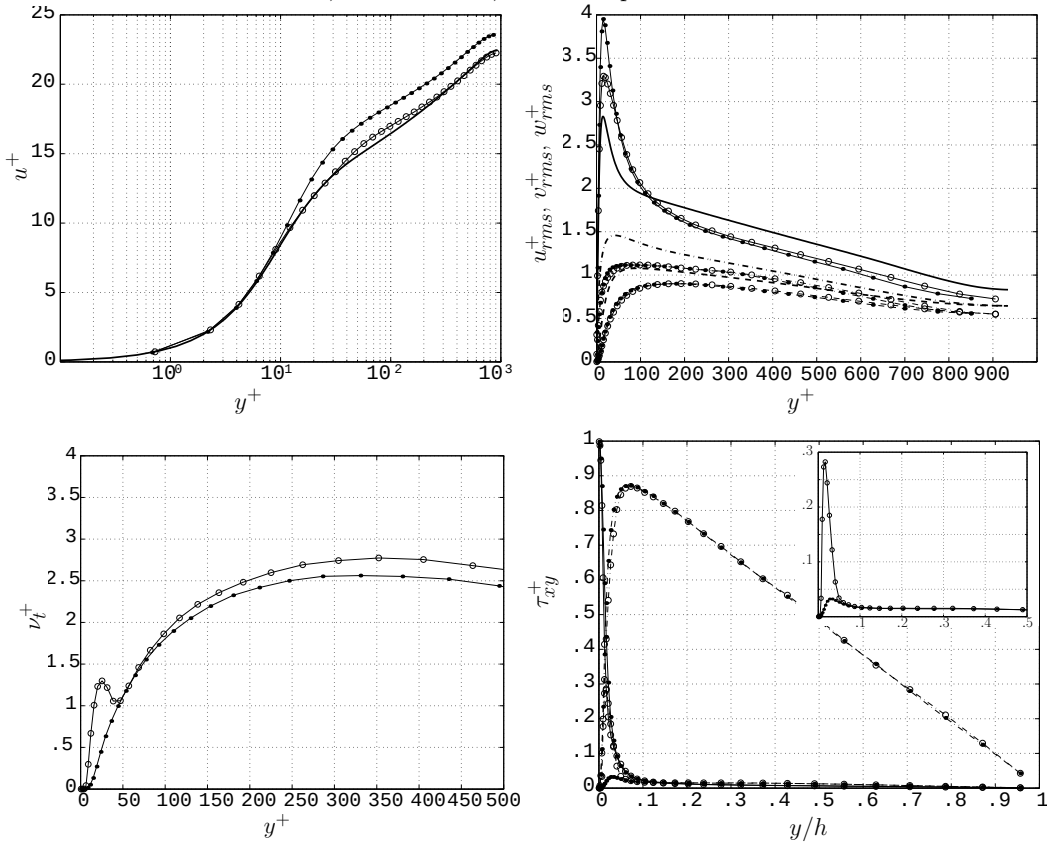

FIGURE 9. Channel flow at $Re_\tau = 950$, $64\times64\times64$ grid. Top: u^+ and rms velocities; Bottom: ν_t^+ and stress balance. LES (•); LES + $\nu_t^{SGS,NW}$ with dynamic coupling with k-ω model equations (○). DNS (solid).

wall eddy-viscosity with the proposed treatment results in an increase in the modeled component in the near-wall region, as shown in the detail of the stress balance plot.

At these Reynolds numbers, the savings in CPU time for wall-parallel coarsening are about one order of magnitude, when compared to full LES. This indicates that wall-parallel coarsening used with the proposed near-wall treatment may be a viable technique for performing LES at lower cost.

6. Conclusions

The RANS/LES coupling formulation proposed in Kalitzin *et al.* (2005b), Medic *et al.* (2005) and Templeton *et al.* (2005) has been adapted for use with various RANS and LES models. The formulation consists of imposing a RANS eddy-viscosity dynamically corrected with the resolved turbulent stress near the wall.

The RANS eddy-viscosity can either be precomputed or obtained by solving the RANS turbulence model equations simultaneously. Results obtained for channel flow at $Re_\tau = 395$ indicate that the near-wall treatment with the dynamic coupling with the Spalart-Allmaras and k-ω model equations is a viable technique. The advantage of the dynamic coupling is in the direct use of the averaged LES velocity field in the solution of the

turbulence model equations. Thus, the RANS eddy-viscosity adjusts to the LES velocity field.

The influence of the subgrid scale model has also been analyzed for channel flow at $Re_\tau = 395$. In addition to the WALE model, the computations were also performed with both the dynamic and the "classical" Smagorinsky model (with constant coefficient C_s). The results obtained with the dynamic Smagorinsky model are very similar to the results obtained with the WALE model. If the near-wall region is extended to $y/h = 0.2$, the computations that employ "classical" Smagorinsky model also yield good results.

The computational advantage of the proposed dynamic coupling was demonstrated on wall-resolved grids coarsened in wall-parallel directions. The results for the channel flow at $Re_\tau = 950$ on a grid with $64 \times 64 \times 64$ cells showed a good agreement with the DNS results, while the traditional LES on the same grid performed poorly. These results indicate that the proposed near-wall coupling can be used with wall-parallel coarsening to perform LES at a reduced cost. The application of the proposed framework to complex flows such as flow in a serpentine passage and flow over a periodic hill is currently under way.

7. Appendix 1: RANS turbulence models

7.1. *Spalart-Allmaras model*

The Spalart & Allmaras (1994) model consists of one transport equation:

$$\partial_t \tilde{\nu} + u \cdot \nabla \tilde{\nu} = Q(\tilde{\nu}) + \frac{c_{b2}}{c_{b3}} \nabla \tilde{\nu} \cdot \nabla \tilde{\nu} + \frac{1}{c_{b3}} \nabla \cdot [(\nu + \tilde{\nu}) \nabla \tilde{\nu}], \tag{7.1}$$

where the source term $Q(\tilde{\nu})$ is

$$Q(\tilde{\nu}) = c_{b1}(1 - f_{t2}) \tilde{S} \tilde{\nu} + \left(\frac{c_{b1}}{\kappa^2} f_{t2} - c_{w1} f_w\right) \left(\frac{\tilde{\nu}}{d}\right)^2. \tag{7.2}$$

The eddy-viscosity is

$$\nu_t = \tilde{\nu} f_{v1}. \tag{7.3}$$

The model damping functions, auxiliary relations and the trip term are defined as

$$f_{v1} = \frac{\chi^3}{\chi^3 + {c_{v1}}^3}, \quad f_{v2} = 1 - \frac{\chi}{1 + \chi f_{v1}}, \quad \chi = \frac{\tilde{\nu}}{\nu}, \tag{7.4}$$

$$f_w = g \left[\frac{1 + {c_{w3}}^6}{g^6 + {c_{w3}}^6}\right]^{\frac{1}{6}}, \quad g = r + c_{w2}(r^6 - r), \quad r = \frac{\tilde{\nu}}{\tilde{S} \kappa^2 d^2}, \tag{7.5}$$

$$\tilde{S} = S + \frac{\tilde{\nu}}{\kappa^2 d^2} f_{v2}, \quad S = \sqrt{2 S_{ij} S_{ij}}, \quad f_{t2} = c_{t3} \exp(-c_{t4} \chi^2). \tag{7.6}$$

The variable d is the distance to the nearest wall, κ the von Kármán constant and the strain rate tensor is $S_{ij} = \frac{1}{2}(\partial_j u_i + \partial_i u_j)$. Finally, the model closure coefficients are

$$c_{b1} = 0.1355, \quad c_{b2} = 0.622, \quad c_{b3} = 2/3, \quad c_{v1} = 7.1, \tag{7.7}$$

$$c_{w1} = \frac{c_{b1}}{\kappa^2} + \frac{1 + c_{b2}}{c_{b3}}, \quad c_{w2} = 0.3, \quad c_{w3} = 2, \quad c_{t3} = 1.2, \quad c_{t4} = 0.5. \tag{7.8}$$

The wall boundary condition is:

$$\tilde{\nu} = 0. \tag{7.9}$$

k-ω model

In the original k-ω model (Wilcox (1993)), the eddy-viscosity is defined as

$$\nu_t = k/\omega. \tag{7.10}$$

The equation for turbulent kinetic energy is

$$\partial_t k + u \cdot \nabla k = P_k - C_\mu \omega k + \nabla \cdot [(\nu + \sigma_k \nu_t)\nabla k], \tag{7.11}$$

where

$$P_k = \nu_t S^2, \qquad S = \sqrt{2 S_{ij} S_{ij}}. \tag{7.12}$$

The equation for the specific dissipation rate ω is:

$$\partial_t \omega + u \cdot \nabla \omega = \frac{\gamma \omega}{k} P_k - \beta \omega^2 + \nabla \cdot [(\nu + \sigma_\omega \nu_t)\nabla \omega]. \tag{7.13}$$

The model constants are

$$\sigma_k = \sigma_\omega = 0.5;\ \gamma = 5/9;\ \beta = 0.075;\ C_\mu = 0.09.$$

The wall boundary condition for k is $k = 0$. At the wall, the specific dissipation rate ω asymptotically tends to infinity as $\sim 1/y^2$. The boundary condition used here is

$$\omega = \frac{60\nu}{\beta d_1^2}, \tag{7.14}$$

where d_1 is the distance from the wall to the cell center of the first cell above the wall.

8. Appendix 2: LES SGS models

8.1. *Wall adapting local eddy-viscosity model (WALE)*

The WALE subgrid-scale model developed by Nicoud & Ducros (1999) is an eddy-viscosity model based on the square of the velocity gradient tensor and accounts for the effects of both the strain and the rotation rate to obtain the local eddy-viscosity. It recovers the proper y^3 near-wall scaling for the eddy-viscosity without requiring a dynamic procedure.

The WALE model eddy-viscosity is given by

$$\nu_t = (C_w \Delta)^2 \frac{\left(\mathcal{S}_{ij}^d \mathcal{S}_{ij}^d\right)^{3/2}}{\left(\overline{S}_{ij}\overline{S}_{ij}\right)^{5/2} + \left(\mathcal{S}_{ij}^d \mathcal{S}_{ij}^d\right)^{5/4}}, \tag{8.1}$$

where $\overline{S}_{ij}$ is the strain rate tensor for the resolved field. $\mathcal{S}_{ij}^d$ is defined as

$$\mathcal{S}_{ij}^d = \frac{1}{2}\left(\overline{g}_{ij}^2 - \overline{g}_{ji}^2\right) - \frac{1}{3}\delta_{ij}\overline{g}_{kk}^2, \tag{8.2}$$

with $\overline{g}_{ij}^2 = \frac{\partial \overline{u}_i}{\partial x_k}\frac{\partial \overline{u}_k}{\partial x_j}$ and δ_{ij} the Kronecker symbol. The model constant $C_w = 0.5$ was calibrated numerically in Nicoud & Ducros (1999) on isotropic decaying turbulence. The subgrid characteristic length scale Δ is set to the cubic root of the local cell volume.

Dynamic Smagorinsky model (DSM)

The eddy-viscosity is given by

$$\nu_t = (C_s \Delta)^2 |\overline{S}_{ij}|, \tag{8.3}$$

where $\overline{S}_{ij}$ is the strain rate tensor for the resolved field and Δ is the effective grid spacing. When the dynamic model is used, the exact definition of Δ is not needed as the total

model parameter $C_s\Delta$ is computed dynamically using the identity of Germano *et al.* (1991) and the least-square approximation of Lilly (1992).

"Classical" Smagorinsky model (DSM)

The eddy-viscosity is given by equation (8.3) with $C_s = 0.18$ and Δ is set to the cubic root of the local cell volume.

Acknowledgments

This research was sponsored by GE Aircraft Engines through the USA program, Belgian American Educational Foundation (BAEF), the AFOSR Grant # F49620-03-1-0132 and by the DOE through the ASC program at CITS.

Computer time was provided by the Center for Research in Aeronautics (CENAERO) which is financially supported by the Walloon region (DGTRE) and the European Union (FEDER and DSE). The second author was visiting the Center for Turbulence Research at Stanford University while this work was performed.

REFERENCES

Baggett, J. S., Jimenez, J. & Kravchenko, A. G. 1997 Resolution requirements in large-eddy simulation of shear flows. *Annual Research Briefs 1997*, Center for Turbulence Research, NASA Ames/Stanford Univ., 51–66.

Balaras, E., Benocci, C. & Piomelli, U. 1996 Two-layer approximate boundary conditions for large-eddy simulations. *AIAA J.* **34**, 1111–1119.

Cabot, W. & Moin, P. 2000 Approximate wall boundary conditions in the large-eddy simulation of high Reynolds number flow. *Flow, Turb. Combust.* **63**, 269–291.

del Alamo, J. C., Jimenez, J., Zandonade, P. & Moser, R. D. 2004 Scaling of the energy spectra of turbulent channels. *J. Fluid Mech.* **500**, 135–144.

Germano, M., Piomelli, U., Moin, P. & Cabot, W. 1991 A dynamic subgrid-scale eddy-viscosity model. *Phys. Fluids* **3**, 1760–1765.

Kalitzin, G., Medic, G., Iaccarino, G. & Durbin, P. A. 2005 Near-wall behavior of RANS turbulence models and implications for wall functions. *J. Comp. Phys.* **204**, 265–291.

Kalitzin, G., Templeton, J. A. & Medic, G. 2005 A near-wall eddy-viscosity formulation for LES. In *Symposium on Complex Effects in Large Eddy Simulation*, Limassol, Cyprus.

Kline, S. J., Reynolds, W. C., Schraub, F. A. & Runstadler, P. W. 1967 The structure of turbulent boundary layers. *J. Fluid Mech.* **30**, 741–773.

Lilly, D. K. 1992 A proposed modification of the Germano subgrid scale closure method. *Phys. Fluids A* **4**, 633–635.

Medic, G., Templeton, J. A. & Kalitzin, G. 2005 A formulation for near-wall RANS /LES coupling. Submitted to *J. Comp. Phys.*

Nicoud, F. & Ducros, F. 1999 Subgrid-scale stress modelling based on the square of the velocity gradient tensor. *Flow, Turb. Combust.* **62**, 183–200.

Nikitin, N. V., Nicoud, F., Wasistho, B., Squires, K. D. & Spalart, P. R. 2000 An approach to wall modelling in large-eddy simulations. *Phys. Fluids. Letters*, **12**, 1629.

Rosenfeld, M., Kwak, D., & Vinokur, M. 1991. A fractional-step solution method

for the unsteady incompressible Navier-Stokes equations in generalized coordinate systems. *J. Comp. Phys.* **94**, 102–137.

Spalart, P. R. & Allmaras, S. R. 1994 A one-equation turbulence model for aerodynamic flows. *La Recherche Aerospatiale* **1**, 1–23.

Spalart, P. R., Jou, W.-H., Strelets, M. & Allmaras, S. R. 1997 Comments on the feasibility of LES for wings, and on a hybrid RANS/LES approach. *First AFOSR Int'l Conference on DNS/LES*, Ruston, LA.

Templeton, J. A., Medic, G. & Kalitzin, G. 2005 An eddy-viscosity based near-wall treatment for coarse grid LES. *Phys. Fluids* **17**.

Wang, M. & Moin, P. 2002 Dynamic wall modeling for large-eddy simulation of complex turbulent flows. *Phys. Fluids* **14**, 2043–2051.

Wilcox, D. C. 1993 *Turbulence modeling for CFD.* DCW Industries, La Canada, CA.

Wu, X. & Durbin, P. A. 2001 Evidence of longitudinal vortices evolved from distorted wakes in a turbine passage. *J. Fluid Mech.* **446**, 199–228.